Linear and nonlinear dynamics of a dust bicrystal consisting of positive and negative dust particles

I. Kourakis[a] and P. K. Shukla[b]
Institut für Theoretische Physik IV and Centre for Plasma Science and Astrophysics, Fakultät für Physik und Astronomie, Ruhr-Universität Bochum, D-44780 Bochum, Germany

G. E. Morfill[c]
Max-Planck Institut für Extraterrestrische Physik, Giessenbachstrasse, D-85740 Garching, Germany

(Received 11 July 2005; accepted 6 October 2005; published online 22 November 2005)

A dusty plasma crystalline configuration consisting of charged dust grains of alternating charge sign $(\cdots/+/-/+/-/+/\cdots)$ and mass is considered. Both charge and mass of each dust species are taken to be constant. Considering the equations of longitudinal motion, a dispersion relation for linear longitudinal vibrations is derived from first principles and then analyzed. Two harmonic modes are obtained, namely, an acoustic mode and an inverse-dispersive optic-like one. The nonlinear aspects of acoustic longitudinal dust grain motion are addressed via a generalized Boussinesq (and, alternatively, a generalized Korteweg–de Vries) description. © *2005 American Institute of Physics*. [DOI: 10.1063/1.2130693]

I. INTRODUCTION

One of the most appealing novel characteristics of dusty (complex) plasmas[1,2] is the occurrence of strongly coupled dust configurations, due to the strong electrostatic interaction between massive, heavily charged dust particulates ("grains"), which exceeds in strength the average dust grain kinetic energy. Spontaneous formation of crystalline-like periodic arrangements is thus observed, typically in the sheath region (above the negative electrode) in gas discharge experiments. Crystal formation and dynamics have been studied in various experiments,[3–5] in which "dust" particles were essentially created by injecting artificial (e.g., formaldehyde) microspheres, which subsequently acquire a high (negative, usually) electron charge via inherent dynamic charging mechanisms. More recent experimental studies have been devoted to positive *and* negative dust charge coexistences in the plasma.[6] Interestingly, studies of alternating charge sign (positive-negative) ionic colloidal crystalline configurations have also recently been reported.[7]

This study is devoted to an investigation, from first principles, of the dynamics of a one-dimensional dust bilayer, consisting of negative and positive dust grains. The principal aspects of harmonic (linear) low amplitude vibrational motion (dispersion laws and eigenmodes) are presented, and a basis for the modeling of larger amplitude, nonlinear motion is proposed, by establishing a link to standard [namely, generalized Boussinesq (GBq) and extended Korteweg–de Vries (EKdV)] nonlinear theories.

[a]Electronic mail: ioannis@tp4.rub.de; URL: http://www.tp4.rub.de/~ioannis
[b]Electronic mail: ps@tp4.rub.de; URL: http://www.tp4.rub.de/~ps
[c]Electronic mail: gem@mpe.mpg.de

II. A DUST BICRYSTAL MODEL

A. Formulation of the problem

We consider a *one-dimensional* horizontal chain (assumed infinite, for simplicity) consisting of negative and positive dust grains, located at equidistant sites (lattice constant r_0). Odd (even) sites, i.e., at $x=(2n+1)r_0$ (or $x=2nr_0$, respectively; $n \in \mathcal{N}$), are occupied by negative (positive) charge dust grains, of charge $-Q_1$ $(+Q_2)$ and mass M_1 $(M_2$, respectively); we assume that $M_1 > M_2$, with no loss of generality. Vertical force equilibrium is ensured by (a balance between) gravity and electric/magnetic forces; only longitudinal displacement $\delta x_n = x_n - nr_0$ (where $n \in \mathcal{N}$) is permitted in this simplified model.

B. Intergrain interactions

The electrostatic binary interaction force $F(r)$ exerted on two grains situated at a distance r is derived from a potential function $U(r)$; viz., $F(r) = -\partial U(r)/\partial x$. Considering the (attractive) interaction between first neighbors only, i.e., $r_{n,n+1} = x_{n+1} - x_n = r_0 + \delta x_{n+1} - \delta x_n$, we may Taylor expand $U(r)$ around r_0 to account for grain displacements. Near the equilibrium configuration, at $r=r_0$ (which is ensured by neighboring grain contributions on both sides around each site), we formally have

$$F(r) \approx -U''(r_0)(r-r_0) - \frac{1}{2}U'''(r_0)(r-r_0)^2 - \frac{1}{6}U''''(r_0)(r-r_0)^3,$$

where the prime denotes differentiation. In the following, we shall set

$$U''(r_0) = G, \quad U'''(r_0)/2 = GA, \quad U''''(r_0)/6 = GB.$$

The description of our dust crystal dynamics is thus effectively reduced to a problem of longitudinal atom motion in a

diatomic chain, characterized by an anharmonic coupling "spring" potential, viz.,

$$U(r) \approx \frac{1}{2}U''(r_0)(r-r_0)^2 + \frac{1}{6}U'''(r_0)(r-r_0)^3 + \frac{1}{24}U''''(r_0)(r-r_0)^4 \equiv G\left[\frac{1}{2}(r-r_0)^2 + \frac{1}{3}A(r-r_0)^3 + \frac{1}{4}B(r-r_0)^4\right]. \quad (1)$$

Our dust bilayer may therefore be analyzed by making use of standard analytical tools from solid-state physics.[8–10]

The model expressions above, in addition to the formulas derived in the forthcoming sections, imply no particular assumption for the potential form $U(r)$. For the sake of clarity, one may consider a "dressed" Debye-type interaction potential-energy function[2,11]

$$U_{drD}(r) = -Q_1Q_2\frac{e^{-r/\lambda_D}}{r}\left(1-\frac{r}{2\lambda_D}\right) \equiv -\frac{Q_1Q_2}{\lambda_D}\frac{e^{-\kappa r'}}{\kappa r'}\left(1-\frac{\kappa r'}{2}\right), \quad (2)$$

where we have defined the lattice parameter $\kappa = r_0/\lambda_D$ and the reduced (dimensionless) space variable $r' = r/r_0$ (recall that $Q_{1,2} > 0$ are the absolute values of the opposite charges here). We note that the potential form (2), introduced in Refs. 11, takes into account the polarization of the Debye sheath around the dust grains; notice, nevertheless, that ion wake and dust grain-size effects are, e.g., neglected, so a different potential form may readily be used in the forthcoming formulas if a more refined description is anticipated. For the potential form (2), one finds

$$U'_{drD}(r_0) = (Q_1Q_2/\lambda_D^2)e^{-\kappa}(1+\kappa-\kappa^2/2)/\kappa^2,$$

$$U''_{drD}(r_0) = -(2Q_1Q_2/\lambda_D^3)e^{-\kappa}(1+\kappa+\kappa^2/2-\kappa^3/4)/\kappa^3 \equiv G,$$

$$U'''_{drD}(r_0) = +(6Q_1Q_2/\lambda_D^4)e^{-\kappa}(1+\kappa+\kappa^2/2+\kappa^3/6-\kappa^4/12)/\kappa^4 \equiv 2GA,$$

$$U''''_{drD}(r_0) = -(24Q_1Q_2/\lambda_D^5)e^{-\kappa}(1+\kappa+\kappa^2/2+\kappa^3/6+\kappa^4/24-\kappa^5/48)/\kappa^5 \equiv 6GB.$$

The ("anharmonic spring") coupling potential which results from the dressed Debye electrostatic interaction law (2) is depicted in Fig. 1, note the asymmetry, due to the strong cubic contribution. The characteristic coefficients involved in it, in fact, functions of the lattice parameter κ, are plotted in Fig. 2. The typical set of values to be retained for reference are for $\kappa=4.5$, $G=8.58\times10^{-4}Q_1Q_2/\lambda_D^3$, $A=+0.097\lambda_D^{-1}$, and $B=-0.045\lambda_D^{-2}$; for $\kappa=5.5$, one has $G=4.9\times10^{-4}Q_1Q_2/\lambda_D^3$, $A=-0.012\lambda_D^{-1}$, and $B=+0.0048\lambda_D^{-2}$ (notice the change in sign, cf. Fig. 2). Note that the stability requirement $Q = U''_{drD}(r_0) > 0$ here imposes $\kappa > 3.4798$.

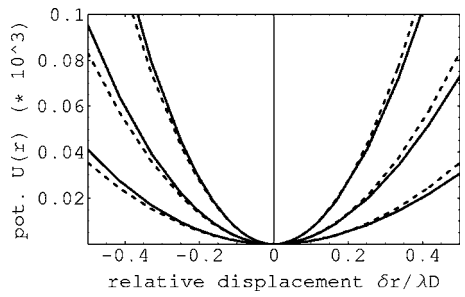

FIG. 1. The anharmonic intergrain coupling ("spring") potential $U(r)$ (normalized by Q_1Q_2/λ_D), as results from Eq. (1) for the dressed Debye electrostatic interaction potential form (2) is depicted vs the reduced relative grain displacement $\delta r/\lambda_D$ (where $\delta r = r_n - r_{n-1}$), for different values of the lattice parameter $\kappa = r_0/\lambda_D$: $\kappa=5$ (upper solid curve), $\kappa=6$ (upper solid curve), and $\kappa=7$ (lower solid curve). The harmonic limit is provided by the parabolas (dashed curves) depicted for comparison. Note the asymmetry (upon $r \to -r$) due to the strong (negative) cubic contribution in $U(r)$.

C. Equations of motion

Denoting the odd (even) grain displacement, within the nth pair, by $\delta z_{2n+1} = z_n$ ($\delta z_{2n} = w_n$), the resulting equations of motion read

$$M_1\frac{d^2z_n}{dt^2} = G(w_n - 2z_n + w_{n-1}) + GA[(w_n-z_n)^2 - (z_n-w_{n-1})^2] + GB[(w_n-z_n)^3 - (z_n-w_{n-1})^3], \quad (3)$$

$$M_2\frac{d^2w_n}{dt^2} = G(z_{n+1} - 2w_n + z_n) + GA[(z_{n+1}-w_n)^2 - (w_n-z_n)^2] + GB[(z_{n+1}-w_n)^3 - (w_n-z_n)^3].$$

Recall that only first-neighbor contributions were considered, due to the fast spatial decay of electrostatic coupling, due to (Debye) charge screening.

III. LINEAR VIBRATIONS

Assuming a plane-wave solution in the form $z = Z\exp i[(2n+1)kr_0 - \omega t] + \text{c.c.}$ (for the heavy negative grains) and $w = W\exp i(2nkr_0 - \omega t) + \text{c.c.}$ (for the lighter positive grains), one finds that the longitudinal vibration

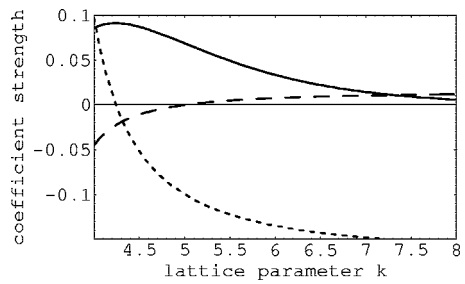

FIG. 2. The value of the (coupling potential expansion) coefficients (for a Debye electrostatic potential) is depicted vs the lattice parameter $\kappa = r_0/\lambda_D$. The coefficients are G (harmonic potential "spring constant:" upper, continuum curve), A (cubic potential nonlinearity: lower, dot curve), and B (quartic potential nonlinearity: middle, dashed curve). The three coefficients are here normalized by $10^{-2}Q_1Q_2/\lambda_D^3$, λ_D^{-1}, and λ_D^{-2}, respectively. Note that the cubic (quartic) contribution to the dressed Debye potential changes sign at $\kappa=4.24$ (5.01, respectively).

(*phonon*) frequency ω is related to the wave number k via the dispersion relation

$$\left(\frac{M_1\omega^2}{2G}-1\right)\left(\frac{M_2\omega^2}{2G}-1\right)=\cos^2 kr_0. \tag{4}$$

The exact solution for the frequency reads

$$\omega_\pm^2=\frac{G}{\mu}\left(1\pm\sqrt{1-\frac{4\mu^2}{M_1M_2}\sin^2 kr_0}\right), \tag{5}$$

where we have defined the *reduced mass*

$$\mu=\frac{M_1M_2}{M_1+M_2}.$$

This relation defines a twofold dispersion curve.

The lower branch ω_- defines an *acoustic mode*; at low k, it satisfies

$$\omega_-\approx\left(\frac{2G}{M_1+M_2}\right)^{1/2},\quad kr_0\equiv c_0k, \tag{6}$$

and thus both the group velocity $v_{\mathrm{gr},-}=\omega_-'(k)$ and the phase velocity $v_{\mathrm{ph},-}=\omega_-/k$ tend to the (constant) *sound velocity* c_0 for low k.

The upper branch ω_+ defines an *optic mode*; at low k, it satisfies

$$\omega_+\approx\left(\frac{2G}{\mu}\right)^{1/2}=\mathrm{const}, \tag{7}$$

and thus $v_{\mathrm{gr},+}=\omega_+'(k)=0$ and $v_{\mathrm{ph},+}\to\infty$ for long wavelengths $\lambda=2\pi/k$.

The frequency band scanned by the two modes includes $\omega_-\in[0,\sqrt{2G/M_1}]$ and $\omega_+\in[\sqrt{2G/M_2},\sqrt{2G/\mu}]$. We note the appearance of a *forbidden frequency range* between

$$\omega_-(k=\pm\pi/2r_0)=\omega_{-,\max}=\sqrt{2G/M_1}$$

and

$$\omega_+(k=\pm\pi/2r_0)=\omega_{+,\min}=\sqrt{2G/M_2}.$$

Furthermore, we point out that the optic mode ω_+ is characterized by an *inverse* dispersion, since $v_{\mathrm{gr},+}=\omega_+'(k)\leqslant 0$ everywhere in the first Brillouin zone (1BZ) $[0,\pi/2r_0]$. It may, however, be pointed out, for rigor, that both of the latter two features (the existence of the forbidden frequency range and the inverse-dispersive character of the optic branch) owe their validity to the assumptions underlying our model (mainly, the absence of second or higher neighbor interactions) and might be modified in a more refined model (if so required by experimental results). The dispersion curve is depicted in Fig. 3.

The amplitude eigenmodes—i.e., the solutions of the linearized system of Eqs. (1), for Z and W—satisfy the relation

$$\frac{W}{Z}=\frac{2G-M_2\omega_\pm^2}{2G\cos kr_0}. \tag{8}$$

The amplitude ratio W/Z is depicted in Fig. 4. We note that *in-phase* (*out-of-phase*) oscillatory dust grain motion is prescribed for long-wavelength acoustic (optic) vibrations, since $W/Z\to 1$ ($W/Z\to -M_2/M_1$, respectively) for $k\to 0$.

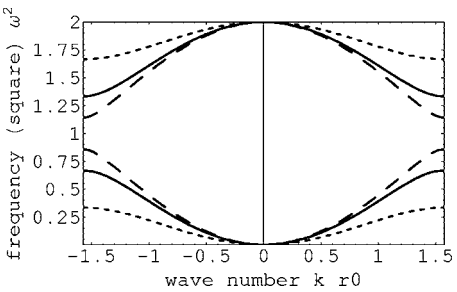

FIG. 3. The dust bilayer dispersion relation: the (square of the) harmonic vibration frequency, i.e., $\omega_\pm^2$ (normalized by G/μ), is depicted vs the reduced wave number kr_0, for a set of indicative (arbitrary) values. Here $G=1$, $M_1=1$, and $M_2/M_1=1/2$ (continuum curve), $M_2/M_1=1/5$ (short-dashed curve), and $M_2/M_1=0.75$ (long-dashed curve). The acoustic (lower) and optic (upper) curves would join at the edge of the first Brillouin zone, for $M_1=M_2$.

IV. CONTINUUM APPROXIMATION

Assuming a long excitation extension $L\gg r_0$, one may substitute the discrete space variables $z_n(t)$ and $w_n(t)$ with continuous ones, say, $z(x,t)$ and $w(x,t)$, by Taylor expanding, i.e.,

$$z_{n\pm1}\approx z\pm 2r_0z_x+2r_0^2z_{xx}\pm\frac{4}{3}r_0^3z_{xxx}+\frac{2}{3}r_0^4z_{xxxx}+\mathcal{O}[(2r_0/L)^5] \tag{9}$$

(plus an analogous expression for $w_n\to w$), where the subscript denotes differentiation, e.g., $z_x=\partial z/\partial x$ and so forth. Inserting into the discrete equations of motion (3), one thus obtains two coupled partial derivative equations (PDEs).

In principle, any analytical approach should be based on a set of coupled evolution equations. However, significant simplification may be achieved by employing a method suggested in Ref. 12 and further elaborated in Refs. 9 and 10. This technique consists of neglecting one of the evolution equations by employing the *Büttner ansatz*[9,10,12]

$$w\approx\sigma\left[z+b_1r_0z_x+\frac{b_2}{2}r_0^2z_{xx}+\frac{b_3}{6}r_0^3z_{xxx}+\frac{b_4}{24}r_0^4z_{xxxx}+b_0f(z)\right]+\mathcal{O}(\epsilon^5). \tag{10}$$

Here σ is set equal to $\sigma_-=1$ ($\sigma_+=-M_1/M_2$) for the acoustic

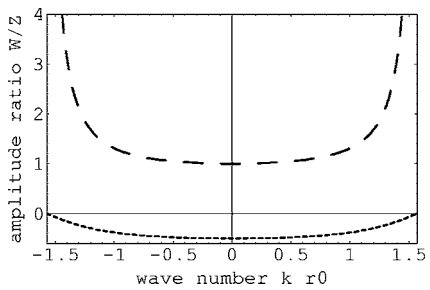

FIG. 4. The amplitude ratio W/Z, as given by (8), is depicted against the reduced wave number kr_0, for a set of indicative (arbitrary) values. Here $G=1$, $M_1=1$, and $M_2/M_1=1/2$. The upper (lower) curve, taking positive (negative) values, corresponds to the acoustic (optic) mode.

(optic, respectively) mode, and the parameters b_j and the function $f(z)$ are appropriately adjusted for compatibility. One thus remains with *one* PDE, in terms of $z(x,t)$, while $w(x,t)$ is defined accordingly (via the ansatz above).

In the following, we shall present some exact results regarding the acoustic mode. The optic mode cannot be studied in this manner,[13] so the corresponding analysis needs to be based on a set of coupled nonlinear evolution equations. This investigation, which goes beyond our scope here, may be the object of further envisaged work, in particular, if forthcoming experiments offer the necessary motivation.

V. NONLINEAR ANALYSIS: THE ACOUSTIC MODE

The compatibility among the equations of motion is ensured by choosing[9]

$$b_0 = 0, \quad \sigma = b_1 = 1, \quad b_2 = 2\mu/M_2,$$

$$b_3 = 6\mu\frac{2M_1 - M_2}{3M_1M_2}, \quad b_4 = 24\mu\left(\frac{1}{3M_2} - \frac{b_2^2}{4M_1}\right), \tag{11}$$

(for first-neighbor only interactions); see that an ordinary Taylor expansion (viz., $b_j=1$ for all j) is recovered in the limit $M_1=M_2$.

A. Generalized Boussinesq acoustic soliton theory

Combining the above expressions and employing the continuum approximation, the system of Eqs. (3) reduces to the single nonlinear PDE

$$z_{tt} - c_0^2 z_{xx} = p_0 z_x z_{xx} + q_0 z_x^2 z_{xx} + h_0 z_{xxxx}, \tag{12}$$

or (in an equivalent manner) the generalized Boussinesq equation

$$u_{tt} - c_0^2 u_{xx} = p(u^2)_{xx} + q(u^3)_{xx} + h_0 u_{xxxx}, \tag{13}$$

where we have set $u=z_x$ and

$$p = \frac{p_0}{2} = GA\frac{b_2}{M_1}, \quad q = \frac{q_0}{3} = GB\frac{b_2}{M_1},$$

$$h_0 = \frac{2G}{M_1}r_0^4\left(\frac{b_4}{24} - \frac{b_3}{6} + \frac{b_2}{2} - \frac{1}{3}\right),$$

while the sound velocity c_0 was defined in (6) above. Recall that compatibility between the two evolutions Eqs. (3) is ensured via Eq. (12) above, which combined with (10) readily provides $w(x,t)$ [for known $z(x,t)$], if necessary.

The well-known Boussinesq equation is recovered from Eq. (13), upon setting $q=0$, or $B=0$, i.e., if one neglects quartic interaction potential contributions. Furthermore, the *modified* Boussinesq equation is recovered from Eq. (13), by setting $p=0$, i.e., $A=0$, thus by neglecting cubic potential contributions. Nevertheless, none of these approximations seem to be appropriate here, since the coefficients p $(\sim A)$ and q $(\sim B)$ bear comparable (absolute) values, in the order of magnitude, as one may check via a simple numerical analysis; as a matter of fact, $|p| \approx 2q$ (viz., $|A| \approx 2B$) for most values of κ (cf. Fig. 2 for A and B). Note that p $[\sim A \sim U'''(r)]$ bears *negative* values for Debye interactions, while q $[\sim B \sim U''''(r)]$ and $h_0 = 2Gr_0^4(m_1^2 - 2m_1m_2 + m_2^2)/[3(m_1+m_2)^3]$ are positive.

The GBq Eq. (13) yields two distinct exact soliton solutions in the form of the *kink* (shock-like) solitons

$$z(x,t) = \pm 2\left(\frac{6h_0}{q_0}\right)^{1/2} \arctan\left[\frac{1}{P_1}\tanh\left(\frac{x - vt}{L_1} + x_0\right)\right], \tag{14}$$

where

$$P_1 = \left[\frac{\sqrt{p_0^2 + 6(v^2 - c_0^2)q_0} \pm p_0}{\sqrt{p_0^2 + 6(v^2 - c_0^2)q_0} \mp p_0}\right]^{1/2}.$$

Here, x_0 and v are real constants, which determine the soliton center and velocity, respectively. Notice that only supersonic excitations are predicted, since $v \geq c_0$. The soliton width is expressed by $L_1 = 2\sqrt{h_0/(v^2 - c_0^2)} \equiv 2\sqrt{h_0}/c_0 \quad (M^2-1)^{-1/2}$ (where M denotes the Mach number $M=v/c_0$). Recall that $L_1 \gg r_0$ in order for the continuum theory to be valid. The two solutions above correspond to a rarefactive and a compressive-localized excitation, propagating in the dust bilayer.

B. Extended KdV acoustic soliton theory

By assuming near-sonic propagation, i.e., $v \approx c_0$, and a very slow time variation (viz., $u_{\tau\tau} \ll u_\tau, u_\xi$), one obtains from the GBq Eq. (13) the canonical form of the extended KdV (EKdV) equation[9]

$$u_\tau + 6uu_\xi + 6u^2u_\xi + u_{\xi\xi\xi} = 0, \tag{15}$$

where we have defined $\xi = p_0(x - c_0t)/\sqrt{6h_0q_0}$, $\tau = p_0^3 t/[2c_0(6q_0)^{3/2}h_0^{1/2}]$, and $u = z_\xi\sqrt{q_0/(6h_0)}$.

The EKdV Eq. (15) was thoroughly studied in a classical series of papers by Wadati,[14] who derived it for nonlinear lattices, then obtained its traveling-wave and periodic (cnoidal wave) solutions, and, finally, exhaustively studied its mathematical properties. Both compressional and rarefactive solitons, say, $u_\pm$, were found to solve Eq. (15). The EKdV Eq. (15) yields two distinct pulse soliton solutions, which may be integrated back to the real displacement z (since $u_\pm = \partial z_\pm/\partial x$) to obtain two distinct kink solitons in the form

$$z_\pm(x,t) = \pm 2\left(\frac{6h_0}{q_0}\right)^{1/2} \arctan\left[\frac{1}{P_2}\tanh\left(\frac{x - vt}{L_2} + x_2\right)\right], \tag{16}$$

where

$$P_2 = \left[\frac{\sqrt{p_0^2 + 12c_0(v - c_0)q_0} \pm p_0}{\sqrt{p_0^2 + 12c_0(v - c_0)q_0} \mp p_0}\right]^{1/2}.$$

The real constants x_2 and v determine the soliton center and (slightly supersonic) velocity, respectively. The soliton width is expressed by $L_2 = 2\sqrt{h_0/[2c_0(v - c_0)]}$. The condition $L_2 \gg r_0$ is assumed to hold in order for the continuum theory to be valid. These two solutions correspond to a rarefactive and compressive-localized excitation. Notice that Eq. (16) is recovered from Eq. (14), by setting $v + c_0 \approx 2c_0$.

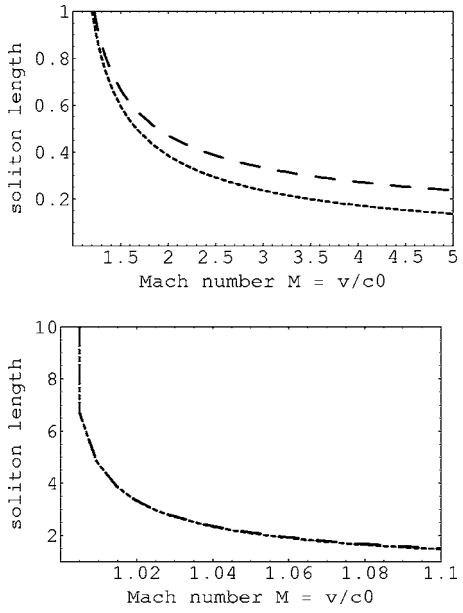

FIG. 5. The (reduced) soliton length L/r_0 is depicted vs the soliton Mach number $M=v/c_0$, as results from the GBq and the EKdV theories: lower (short-dashed) and upper (long-dashed) curves, respectively. The right figure depicts the near-sonic region, i.e., near $M=1$, where the two theories practically coincide.

C. Discussion and comparison

We see that the EKdV-equation-related theory adds no truly extra information to that obtained via the (less approximate) Boussinesq theory. As a matter of fact, the predicted soliton length is slightly higher than its GBq analog (see Fig. 5). We observe that the condition $L/r_0 \gg 1$, which ensures the validity of the continuum approximation, is only valid for velocities slightly above the sound velocity c_0, where the two theories admittedly practically coincide (see Fig. 5). On the other hand, it should be noted that the slow time variation hypothesis, which enables one to reduce the continuum (GBq-related) evolution equation (13) to the EKdV Eq. (15), results in the loss of the time-reversal symmetry, which is inherent in the former equation.

An additional comment concerns the ordinary KdV theory, widely adopted, e.g., for dusty plasma monolayers, since the original work of Melandsø.[15] Indeed, reducing either the GBq or the EKdV to an ordinary KdV (which implies neglecting a quartic potential nonlinearity) results in significant analytical simplification. Nevertheless, the KdV theory only predicts one type of (compressional, in fact, for Debye interactions) excitations, contrary to the two types of kink excitations predicted above. This fact is simply due to the *sign* of the nonlinear term in the KdV equation being prescribed as *negative* for Debye interactions. An extended discussion on this respect, from first principles, is carried out in Ref. 16, as regards the longitudinal dust lattice solitons in one-component dust crystals, so we need not reproduce those arguments here.

The kink soliton solutions which result from the GBq Eq. (13) and the EKdV Eq. (15), as given by Eqs. (14) and (16), respectively, are depicted in Figs. 6 and 7 for near-sonic ($v=1.2c_0$) and highly supersonic ($v=3c_0$) propagations, respectively. Note that the kink soliton is higher than its antikink analog for low velocity v [cf., e.g., Figs. 6(a) and 7(a)]. Also note that the higher velocity results in narrower solitons, as prescribed by the theory. Finally, notice that the two theories practically coincide for v near the sound velocity c_0 [see Fig. 6(c)], while the GBq solitons are steeper (narrower) for higher propagation velocity v [cf. Fig. 7(c)].

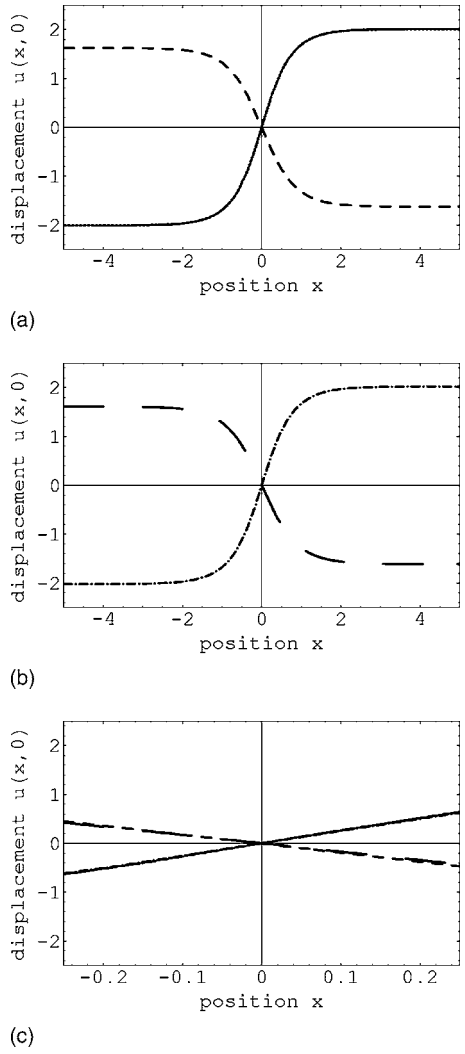

FIG. 6. (a) The GBq kink solitons (dust grain displacement), as defined in Eq. (14), are depicted vs position x (for $x_0=t=0$): kink (continuous curve), antikink (short-dashed curve); (b) the EKdV kink solitons (dust grain displacement), as defined in Eq. (16), are depicted vs position x (for $x_2=t=0$): kink (dot-dashed curve), antikink (long-dashed curve); and (c) all four soliton solutions: detail near the origin. Here, we have assumed Debye interactions with $\kappa=1$, Mach number $M=v/c_0=1.2$; also, $m_1=2m_2=1$, $G=r_0=1$ (arbitrary values).

VI. CONCLUSIONS

This study was devoted to a first investigation, from first principles, of the dynamics of a one-dimensional dust bilayer, consisting of negative and positive dust grains. The main aspects of harmonic (linear) longitudinal motion were presented, and a dispersion relation was derived and analyzed. An analytical model for a larger amplitude, nonlinear motion was proposed, thus establishing a link to standard [in

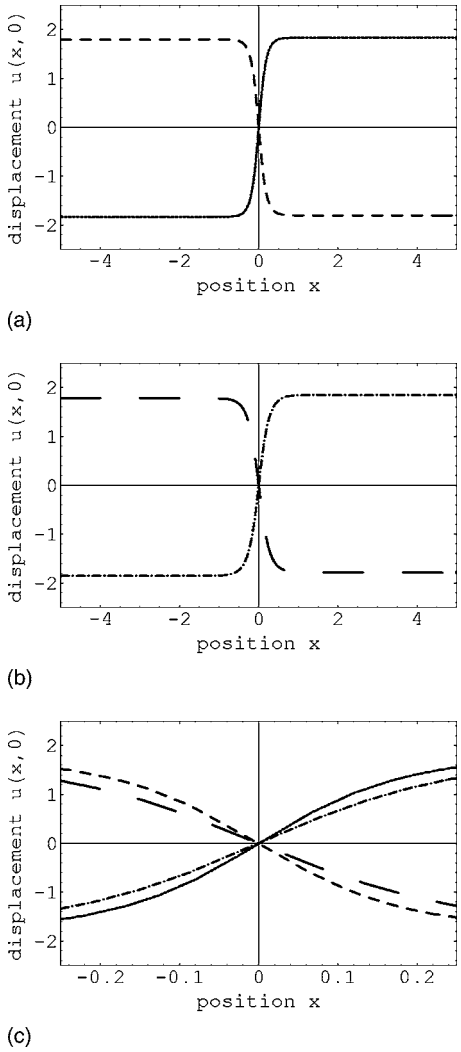

FIG. 7. Similar to Fig. 6, for $M=3$ (all other parameter values are identical). (a) The GBq kink solitons (dust grain displacement), as defined in Eq. (14), are depicted vs position x (for $x_0=t=0$): kink (continuous curve), antikink (short-dashed curve); (b) the EKdV kink solitons (dust grain displacement), as defined in Eq. (16), are depicted vs position x (for $x_2=t=0$): kink (dot-dashed curve), antikink (long-dashed curve); and (c) all four soliton solutions: detail near the origin. Here, we have assumed Debye interactions with $\kappa=1$, Mach number $M=v/c_0=3$; also, $m_1=2m_2=1$, $G=r_0=1$ (arbitrary values).

specific, the generalized Boussinesq (GBq) and extended Korteweg–de Vries (EKdV)] nonlinear theories.

Both nonlinear theories predict two types of supersonic shock-shaped kink excitations, corresponding to a localized compression and a rarefaction, respectively, propagating in the dust bilattice. The two theories practically coincide for a propagation velocity near the sound speed but diverge significantly far from it. The spatial extension of the soliton decreases with its speed, so faster solitons are steeper. Similar results have been obtained for one-dimensional dust monolayers.[16] Finally, we have carried out a brief critical discussion of the two theories employed here (based on the generalized Boussinesq and the extended Korteweg–de Vries equations), which take into account nonlinearities up to the fourth order, in comparison with the ordinary Korteweg–de Vries equation, which only accounts for compressional excitations, for Debye interactions (cf. the extended discussion in Ref. 16).

These theoretical considerations and quantitative predictions will hopefully be confirmed by appropriately designed experiments.

ACKNOWLEDGMENTS

One of the authors (I.K.) is grateful to B. Farokhi, for his sharp-minded criticism, in addition to a number of enlightening discussions.

This work was partially supported by the Deutsche Forschungsgemeinschaft (Bonn, Germany) through the Sonderforschungsbereich (SFB) 591—Universelles Verhalten Gleichgewichtsferner Plasmen: Heizung, Transport und Strukturbildung.

[1] F. Verheest, *Waves in Dusty Space Plasmas* (Kluwer Academic, Dordrecht, 2001).
[2] P. K. Shukla and A. A. Mamun, *Introduction to Dusty Plasma Physics* (Institute of Physics, Bristol, 2002).
[3] H. Thomas, G. E. Morfill, V. Demmel, J. Goree, B. Feuerbacher, and D. Möhlmann, Phys. Rev. Lett. **73**, 652 (1994); A. Melzer, T. Trottenberg, and A. Piel, Phys. Lett. A **191**, 301 (1994); Y. Hayashi and K. Tachibara, Jpn. J. Appl. Phys., Part 2 **33**, L84 (1994).
[4] G. Morfill, H. M. Thomas, and M. Zuzic, in *Advances in Dusty Plasma Physics*, edited by P. K. Shukla, D. A. Mendis, and T. Desai (World Scientific, Singapore, 1997), p. 99; G. E. Morfill, H. M. Thomas, U. Konopka, H. Rothermel, M. Zuzic, A. Ivlev, and J. Goree, Phys. Rev. Lett. **83**, 1598 (1999).
[5] S. Nunomura, D. Samsonov, and J. Goree, Phys. Rev. Lett. **84**, 5141 (2000).
[6] R. L. Merlino (private communication).
[7] M. E. Leunissen *et al.*, Nature (London) **437**, 235 (2005).
[8] C. Kittel, *Introduction to Solid State Physics* (Wiley, New York, 1996).
[9] St. Pnevmatikos, *Dynamique des Solitons dans les Réseaux Diatomiques Non-linéaires*, Thèse d'Etat (Université de Bourgogne, Dijon, 1984).
[10] St. Pnevmatikos, M. Remoissenet, and N. Flytzanis, J. Phys. C **16**, L305 (1983).
[11] S. Hamaguchi and R. T. Farouki, Phys. Rev. E **49**, 4430 (1994); D. P. Resendes, J. T. Mendonça, and P. K. Shukla, Phys. Lett. A **239**, 181 (1998).
[12] H. Büttner and H. Bilz, in *Solitons and Condensed Matter Physics*, edited by A. R. Bishop and T. Schneider (Springer, Berlin, 1978) pp. 162–165.
[13] As a matter of fact, compatibility of the two evolution equations via the "Büttner ansatz" *cannot* be achieved for asymmetric potentials, i.e., when a cubic contribution is present in the nonlinear potential. This *is* the case in a dust crystal, as results from the analysis of Debye interactions. See in Appendix D, in Ref. 9, for a detailed discussion and analytical expressions.
[14] M. Wadati, J. Phys. Soc. Jpn. **38**, 673 (1975); **38**, 681 (1975).
[15] F. Melandsø, Phys. Plasmas **3**, 3890 (1996).
[16] I. Kourakis and P. K. Shukla, Eur. Phys. J. D **29**, 247 (2004).